

The use of X-ray absorption spectroscopy for speciation studies in cementitious systems

E. Wieland¹, M. Vespa^{1,2}, R. Dähn¹, D. Grolimund¹, A.M. Scheidegger^{1,2}

¹*Paul Scherrer Institut, Villigen PSI, Switzerland;* ²*Swiss Federal Institute of Technology (ETH), Zürich, Switzerland*

Abstract

Cementitious matrices are being used worldwide as a containment medium for hazardous and radioactive waste in order to retard the mobility of contaminants. The development of mechanistic models of immobilization processes in connection with further improvements in the thermodynamic modeling of cementitious systems are regarded as key issues with a view to assessments of the long term impact of cement-stabilized waste on the environment. In the past years synchrotron-based X-ray absorption spectroscopy (XAS) has been applied as local probe to investigate uptake processes in cementitious materials on the molecular level. This information can be used to develop mechanistic models of the interaction of contaminants with the cement matrix. For example, XAS investigations on the Sr uptake by cementitious materials have been carried out. Further, high resolution analytical synchrotron-based X-ray microprobes have been utilized to obtain spatially resolved information on the chemical speciation of Ni immobilized in the cement matrix. In this study we will show how the latter technique can be employed in combination with conventional scanning electron microscopy to determine micro-scale processes in heterogeneous cementitious materials.

1 Introduction

X-ray absorption spectroscopy represents a powerful collection of techniques capable of providing molecular-level information on the coordination environment of an element of interest (e.g., [1, 2]). Most frequently used XAS techniques are X-ray absorption near edge structure (XANES) and extended X-ray absorption fine structure (EXAFS) spectroscopy. While X-ray diffraction (XRD) experiments probe the long-range order of crystalline samples, XAS probes the local environment of an X-ray absorber atom. The method allows non-destructive in-situ speciation measurements to be carried out and the coordination sphere (type of neighboring atoms, bond length and coordination numbers) of the X-ray absorber atom to be determined. Further, the method is capable of distinguishing different oxidation states of the X-ray absorber. Dilute samples can be examined (concentrations down to a few tens of ppm),

and the samples can be in almost any forms (crystalline and amorphous solids, liquid, suspension, or gas). In contrast to diffraction analyses, the method does not require long range ordering (crystalline samples).

Cementitious matrices are being used worldwide as a containment medium for hazardous and radioactive waste in order to prevent or retard the release of contaminants from the waste matrix into the environment [3]. Over the past decade the interest in using XAS to develop a molecular-level understanding of the chemical processes governing the immobilization of contaminants in cementitious materials has been growing (see [4] and references therein). For example, this level of understanding is essential for detailed assessments of the long-term behavior of radionuclides in a cementitious repository for radioactive waste, since chemical processes operative on the molecular level may have large impacts over long time scales. Much of our understanding of the speciation of contaminants in cementitious waste matrices, such as Sr(II), Ni(II), Co(II), Cr(VI/III), Pb(II), Cd(II), Eu(III), Np(V)O₂⁺, U(VI)O₂²⁺, SeO₄²⁻/SeO₃²⁻, AsO₄³⁻, TcO₄⁻, has been gained from XAS studies on crushed materials (see [4] and references therein). XAS has provided new insights into uptake mechanisms on the molecular level. In cementitious systems uptake may be caused by chemical bonding of ions onto surface sites of cement phases, the incorporation of ions in mineral structures, or the formation of secondary solid phases. Thus, XAS has proven to be well suited for investigations of the chemical nature of sorbed (or immobilized) species in complex cement matrices. XAS has further been applied to determine the local coordination of cement-derived elements in these materials in earlier studies (e.g., [5,6]).

Although XAS studies on powder materials is the method of choice for gaining molecular-level information on chemical reactions in complex natural and engineered materials, the application of the method becomes problematic when mechanisms operative on the micro-scale have to be identified. Usually, XAS does not yield spatially resolved structural data since the dimension of the X-ray beam is much bigger (at most beamlines >100 x 100 μm²) than the particle size of minerals under investigation (normally < 20 x 20 μm²). In the latter case, the speciation of a contaminant is determined by the averaged XAS signal from all of the individual species (bulk XAS measurements). To determine micro-scale processes in heterogeneous cementitious materials, however, analytical synchrotron-based X-ray microprobes with high spatial resolution are required, with which the wealth of structural information provided by micro-X-ray absorption spectroscopy (microXAS) can be obtained. Several studies have demonstrated the potential of the synergistic use of micro-X-ray fluorescence (microXRF) and microXAS (see [4] and references therein, [7]). MicroXRF is essential in a first step to map the distribution of contaminants among coexisting mineral phases in the investigated sample. MicroXAS opens up the possibility to determine the chemical speciation of the X-ray absorber of interest on the micro scale.

In this study, bulk XAS measurements and microXRF/XAS studies have been carried out to determine the coordination environment of Sr(II) and Ni(II) in cementitious materials. These investigations are important in conjunction with the safe disposal of radioactive waste. The first example addresses the use of XAS on crushed materials to gain chemical structural information on Sr(II) taken up by cementitious materials. The second example illustrates the potential of using synchrotron-based X-ray microprobe techniques in combination with conventional scanning electron microscopy (SEM) to determine the spatial distribution and speciation of Ni(II) in the cement matrix with micro-scale resolution.

2 XAS investigation on Sr uptake by cementitious materials

Cement contains considerable amounts of Sr. The concentration of pristine (non-radioactive) Sr in cement clinker was found to range in value between about one hundred and more than thousand parts per million (ppm) (e.g., [8] and references therein), depending on the initial Sr concentrations of the raw materials used for cement production. The most important radioactive isotope, ^{90}Sr , which is present in cement-stabilized radioactive waste, belongs to the category of fission products found in operational waste from reactors and reprocessing plants. XAS was applied to elucidate the binding mechanisms of Sr in calcium silicate hydrates (C-S-H) and hardened cement paste (HCP) with the aim of developing a mechanistic model for the radiostrontium immobilization in cement-stabilized radioactive waste.

2.1 Materials and methods

Commercial sulfate-resisting Portland cement denoted as HTS cement (CEM I 52.5 N HTS (= Haute Teneur en Silice), Lafarge, France) was used for the preparation of the Sr doped HCP samples. The concentration of pristine Sr in HTS cement was determined to be 1290 ± 92 ppm. Details of sample preparation are given elsewhere [8]. C-S-H phases (C/S ratios = 0.7 and 1.1) were synthesized and doped with Sr as described in [9].

Sr K-edge (16.105 keV) EXAFS measurements on Sr doped C-S-H and HCP samples and reference compounds were carried out at cryogenic temperatures (15 K, 77 K) to minimize the effect of thermal disorder. The measurements were carried out at BM26 (DUBBLE) (Sr doped C-S-H samples), and at BM01 (SNBL) (references) at the ESRF, Grenoble, France, and at X-11A (Sr doped HCP samples) at NSLS, Brookhaven, USA. Details of the measurements are given elsewhere [8]. EXAFS data reduction was performed using the WinXAS3.11 software package following standard procedures. Theoretical scattering paths were calculated with FEFF8.20 using $\alpha\text{-Ca}_{1.65}\text{Sr}_{0.35}\text{SiO}_4$ as model compound. The fitting approach is described elsewhere [8]. The precision of the structural parameters was estimated to be about ± 0.02 Å for the interatomic distance (R) and about ± 25 % for the coordination number (N).

2.2 Results and discussion

The EXAFS study focused on elucidating the coordination environment of pristine Sr and Sr taken up HCP. It was speculated that differences in the local binding of the different Sr species could appear in the EXAFS data. Thus, HCP was depleted from pristine Sr and reloaded by adding a Sr solution to discern changes in the Sr coordination environment in the treated HCP samples (Cem_LE: HCP leached in Milli-Q water, Cem_HD: half depleted from pristine Sr, Cem_FD: fully depleted from pristine Sr) in comparison with Sr bound in the untreated samples (Cem_U) samples. Details of the sample preparation are given elsewhere [8].

Figure 1 shows the radial structural functions (RSFs) of the Sr doped C-S-H and HCP samples, which were obtained by Fourier transforming k^3 -weighted $\chi(k)$ functions between 2.6 and 10.5 \AA^{-1} .

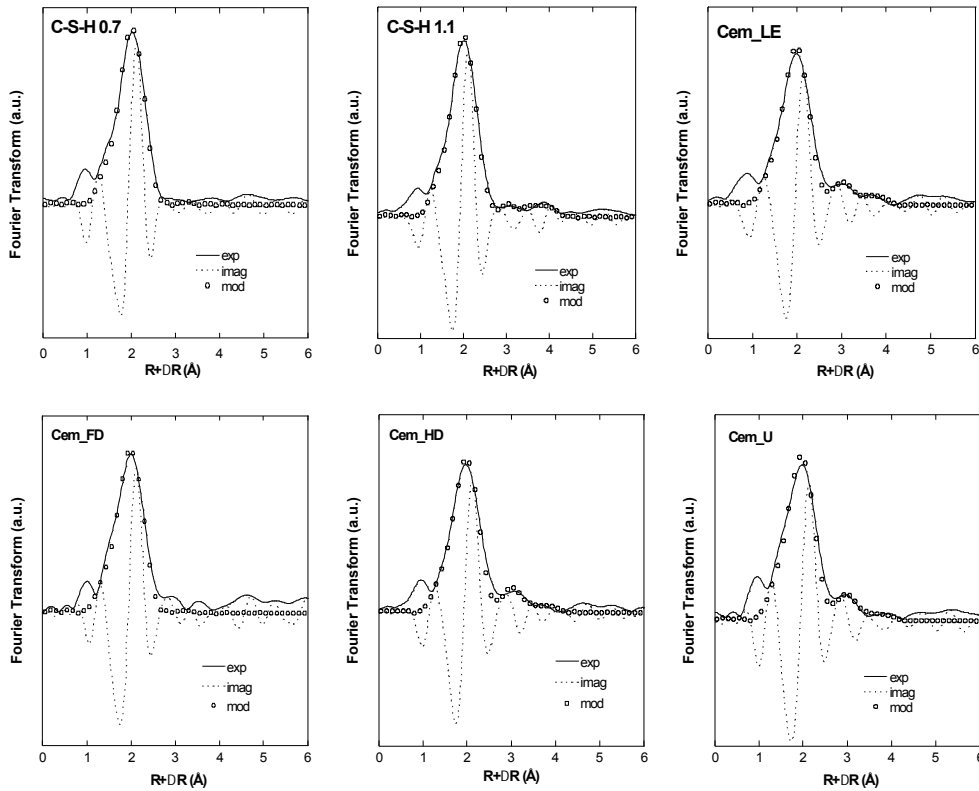


Figure 1 Experimental (solid lines) and theoretical (circles: modulus; dashed: imaginary part) Fourier transforms obtained from Sr K-edge EXAFS of the Sr doped C-S-H and HCP samples (modified from [8]). For sample description see text, and for more details [8].

Table 1 summarizes the structural parameters determined from non-linear least-square fitting of the experimental data in real space ($\Delta R = 0.7 - 5 \text{\AA}$). The EXAFS spectra reported in [8] are not shown for reasons of space.

Table 1 Structural parameters obtained for the Sr doped C-S-H and HCP samples.

Sample		N	R (Å)	$\sigma^2(\text{Å}^2)$	ΔE_0 (keV)	Res (%)
C-S-H 0.7	Sr-O	6.3	2.60	0.008	0.6	6.4
C-S-H 1.1	Sr-O	7.6	2.61	0.009	-0.3	6.6
	Sr-O	1.9	3.68	0.011	-0.3	6.6
	Sr-Si	2.0	4.33	0.011	-0.3	6.6
Cem_U	Sr-O	6.1	2.57	0.012	-0.2	10.7
	Sr-O	2.0	3.59	0.009	-0.2	10.7
	Sr-Si	0.7	4.22	0.009	-0.2	10.7
Cem_HD	Sr-O	6.4	2.58	0.011	0.5	8.4
	Sr-O	1.9	3.61	0.007	0.5	8.4
	Sr-Si	0.7	4.23	0.007	0.5	8.4
Cem_FD	Sr-O	6.4	2.59	0.010	0.0	7.8
Cem_LE	Sr-O	6.8	2.59	0.011	0.8	8.3
	Sr-O	1.8	3.61	0.007	0.8	8.3
	Sr-Si	0.8	4.23	0.007	0.8	8.3

N is the coordination number, R denotes bond distance (Å), σ is the Debye-Waller factor (Å), ΔE_0 the energy shift (eV). The residual factor (%Res) represents the quality of the fit

$$\% \text{ Res} = \frac{\sum_{i=1}^N |y_{\text{exp}}(i) - y_{\text{fit}}(i)|}{\sum_{i=1}^N y_{\text{exp}}(i)} \times 100$$

Comparison of the EXAFS spectra of the Sr doped C-S-H and HCP samples with those of reference compounds, i.e., SrO, Sr(OH)₂, SrCO₃ and SrSO₄, showed that the formation of crystalline solids or any solid solution in these samples can be excluded [8]. The RSFs of all of the samples are dominated by backscattering contributions from the first oxygen shell (R = 2.57-2.60 Å) (Table 1). Variation in the coordination number was found to be within the given uncertainty range (N = 6.1 - 7.6). The Sr-O bond distances were found to be comparable to those determined for the aqueous Sr species under alkaline conditions and Sr(OH)₂ ([8]). The number of first shell oxygen atoms was found to be comparable to that in Sr(OH)₂ (N ~6), but significantly lower than in the aqueous Sr species (N ~9). Backscattering contributions from further shells were found to be very weak or even below the noise level in case of the C-S-H 0.7 and Cem_FD samples (Fig. 1). For the other samples, however, significant improvements in the fits were achieved by taking into

account further neighboring oxygen (~ 2 O at 3.59-3.68 Å) and silica atoms (1 - 2 Si at 4.22-4.33 Å) (Table 1). The presence of the second oxygen and an additional silica shells implies that Sr is bound via bridging oxygen atoms to Si surface sites in HCP and on the surface of the C-S-H phase. For all of the HCP samples data analysis yielded similar structural parameters, suggesting that pristine Sr and Sr added to HCP samples occupy the same structural sites in the cement matrix. Furthermore, the same type of neighboring atoms was determined for the Sr doped HCP and C-S-H samples, suggesting that C-S-H could be the uptake-controlling phases for Sr in the cement matrix. The observed differences in the bond distances and the coordination numbers for Sr in the two types of solids, however, indicate that the local coordination environment of Sr bound to C-S-H and HCP might be slightly different.

3 Microscopic and micro-spectroscopic studies on Ni uptake by cementitious systems

The combination of SEM with synchrotron-based microXRF/XAS has proven to be a very promising approach for spatially resolved micro-scale investigations of the speciation of contaminants in heterogeneous cement matrices (e.g., see [4] and references therein, [7]). SEM-based backscattering electron imaging (BSE) and energy dispersive spectroscopy (EDS) were found to be an essential first step to address questions concerning the microstructure of the cement matrix, to identify the clinker minerals and reactive zones of the hydrate assemblage, and to determine the partitioning of Ni among coexisting mineral phases in the investigated sample. Determination of the spatial distribution of Ni in the cement matrix by microXRF mapping was the first step in the synchrotron-based studies. MicroXAS allowed molecular-level information on the chemical speciation of Ni to be gained. This information was found to be essential in connection with the development of a mechanistic model of Ni immobilization in intact cementitious materials. With the present study on the Ni uptake by solidified hydrated cement it is intended to illustrate the possibility of combining SEM-BSE/EDS with microXRF/XAS on the same region of interest in the given sample.

3.1 Materials and methods

The Ni-doped hydrated cement paste was prepared by mixing a $\text{Ni}(\text{NO}_3)_2$ solution with HTS cement. The final concentration of Ni(II) in the paste was 5000 ppm. Sample preparation is described in detail elsewhere [7]. Slices of the Ni-doped paste hydrated for 30 days were impregnated and polished for the preparation of thin sections. The thin sections were employed for both SEM-BSE/EDS investigations and the synchrotron-based micro-focused XRF/XAS measurements.

SEM investigations were conducted at the Laboratory for Construction Materials (IMX), Ecole Polytechnique Fédérale de Lausanne (EPFL) and at

the Laboratory for Materials Behaviour (LWV) at the Paul Scherrer Institute (PSI). Equipment and experimental details are reported elsewhere [10]. MicroXRF mapping of Ca, Si, Al and S was carried out at the LUCIA beamline at the Swiss Light Source (SLS), Switzerland [11]. MicroXAS spectra at the Ni K-edge (8.333 keV) were collected on beamline 10.3.2 (ALS) with the same setup as for the microXRF maps [12]. Technical details of the measurements are given elsewhere [7, 10].

3.2 Results and discussion

The combination of BSE imaging with EDS microanalysis allows spatially resolved information on the chemical composition of the different mineral phases to be gained (e.g., [13]). Figure 2 shows a BSE image and EDS microanalysis of the Ni-doped hydrated cement matrix.

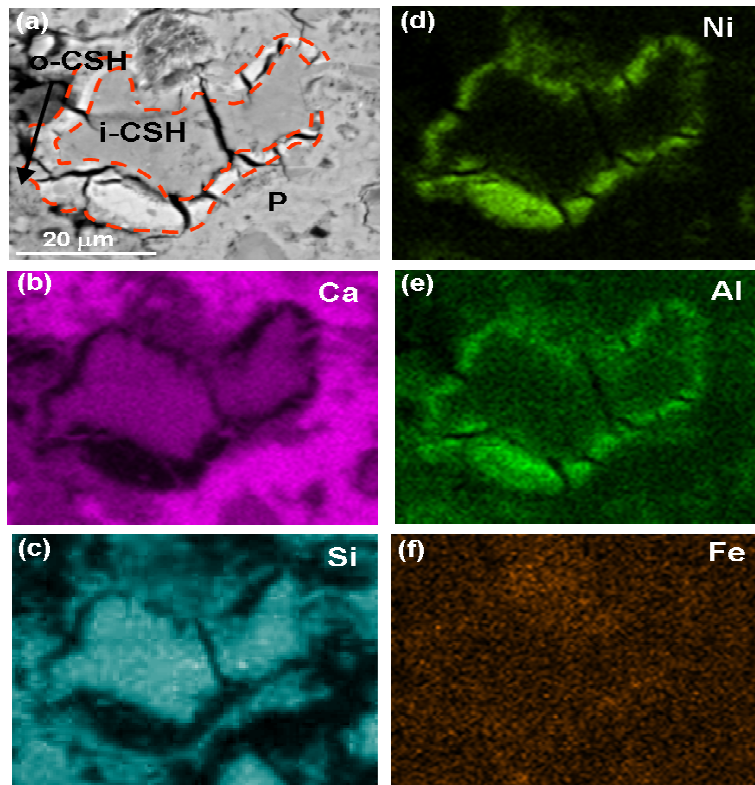


Figure 2 BSE images (a) and SEM-EDS elemental distribution maps (b-f) of a Ni-rich region in Ni-doped HCP samples with a Ni loading of 5000 ppm and hydrated for 30 days. Note that in the SEM-EDS maps (b) to (f) increasing concentrations are indicated by increasing brightness. The red dashed area in (a) represents the Ni-rich region. Notations: P= portlandite ($\text{Ca}(\text{OH})_2$), i-C-S-H=inner-calcium silicate hydrate, o-C-S-H= outer-C-S-H.

The BSE image shows that a bright Ni-rich rim forms around inner-C-S-H, suggesting a direct association with this cement phase. Ni rims of a few

hundred nanometers up to a few micron thicknesses and up to ~20 - 50 μm in diameter were observed. Mapping shows that the Ni distribution is heterogeneous and that Ni correlates only with Al. Note that the maps are based on relative concentrations. Semi-quantitative concentration measurements were obtained from EDS point analysis. The data revealed that the rims also contain Ca and Si, and small amounts of Al [10].

BSE imaging further showed that Ni-rich rims preferentially form around alite [10]. A tentative explanation for this finding can be given by considering some specific features of the mineral. Alite (C_3S) dissolves much faster than belite (C_2S), which allows inner-C-S-H type zones to be rapidly formed around C_3S grains [14]. The reactive zones are expected to have a high specific surface area. Therefore, a large number of surface sites may be exposed for Ni binding, which facilitates Ni accumulation at the grain boundaries of C_3S . It is speculated that, in addition to Ni, Al may accumulate in this zone due to rapid dissolution of C_3A [14]. Accumulation of the main constituents needed to form hydrotalcite-like phases, i.e., Mg and Al, and the Ni contaminant could promote the formation of Ni containing layered double hydroxide (LDH)-type phases.

Nevertheless, SEM-BSE/EDS investigations do not provide further information on the Ni speciation. This information is available from microXRF/XAS. MicroXRF elemental maps were required to gain an overview of the Ni distribution in the cement matrix in order to localize the regions of interest for microXAS measurements (Fig. 3). Fig. 3 shows microXRF maps of Ni and important elements of the cement matrix, i.e., Ca, Si, Al and S, together with a BSE image of the same region. This figure illustrates the heterogeneity of the cement matrix and the heterogeneous distribution of Ni in hydrated cement. In Fig. 4 selected microXAS data of single Ni-rich and Ni-poor spots (marked with 1 and 2, respectively, in Fig. 3) and relevant Ni reference spectra are shown. The microXAS spectra performed on the spots reveal similar features, suggesting a similar coordination environment of Ni at low and high Ni concentrations (Fig. 4). The oscillation at $\sim 4 \text{ \AA}^{-1}$ is broad and is located at a k-range position that agrees with the position of the first major oscillation observed in the spectrum of neo-formed LDH phase (N-LDH). The splitting of the oscillation at $\sim 8 \text{ \AA}^{-1}$ is a characteristic beat pattern, which can be used as fingerprint for Ni-Al LDH (e.g., [7] and references therein). In fact, this beat pattern appears in both Ni-Al LDH spectra (LDH and N-LDH), whereas the other reference compounds ($\alpha\text{-Ni(OH)}_2$, $\beta\text{-Ni(OH)}_2$ and Ni-phylllosilicate) show an elongated upward oscillation ending in a sharp tip at $\sim 8.5 \text{ \AA}^{-1}$. Thus, the presence of the beat pattern at $\sim 8 \text{ \AA}^{-1}$ together with the observed spectral features at $\sim 4 \text{ \AA}^{-1}$ is indicative of the formation of Ni-Al LDH phase formed at the single spots in the Ni-doped cement matrix.

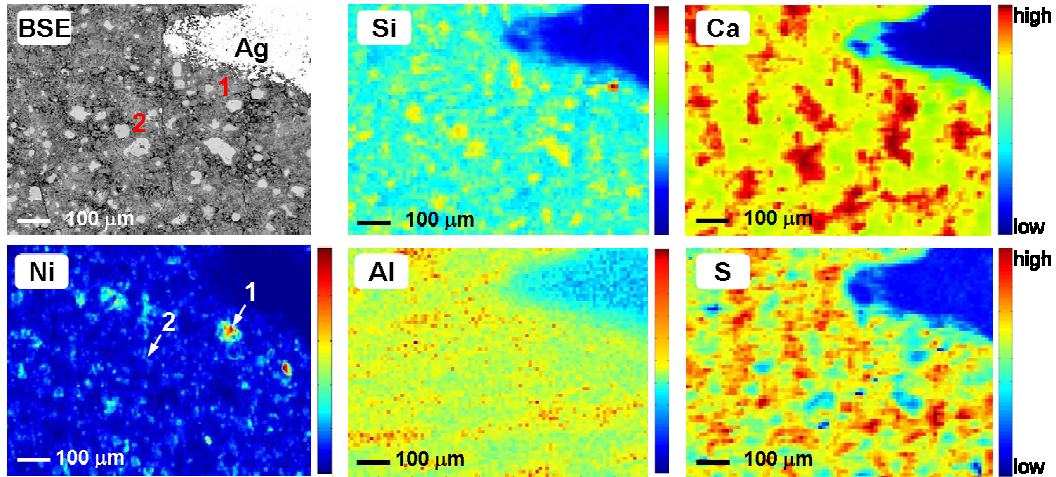


Figure 3 BSE image and microXRF elemental distribution maps of Ni Si, Ca, Al and S in a $1000 \times 1000 \mu\text{m}^2$ overview of the Ni-doped cement matrix. MicroXAS selected regions for Ni K-edge measurements are marked with numbers (1, 2) on the BSE image and the Ni map. Ag = silver spot used as marker, which appears blue on the microXRF maps.

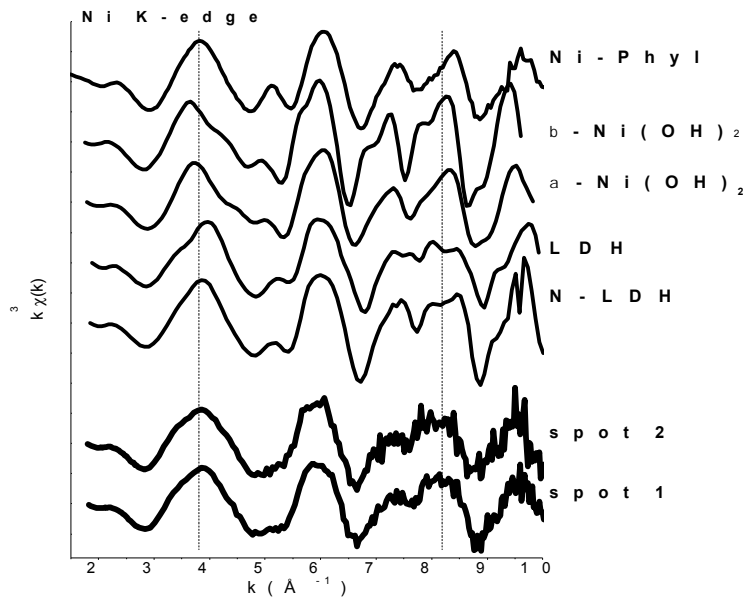


Figure 4 Ni K-edge k^3 -weighted, normalized, background-subtracted spectra of reference compounds and spectra collected at spot 1 and 2 (Fig. 3) of the Ni-doped sample (5000 ppm). Dashed lines indicate spectral features explained in the text. Notations: N-LDH = neo-formed Ni-Al LDH, LDH = synthetic Ni-Al LDH (Ni:Al, 2:1), Ni-Phyl = Ni-phyllsilicate.

More detailed analysis of the EXAFS spectra was carried out by multi-shell fitting to determine the structural parameters of the Ni compounds. These data, which are shown together with the corresponding RSFs elsewhere [10], further supported the idea that Ni-Al LDH formed in the given sample.

4 Conclusions

XAS is a local probing technique which provides molecular-level information on the chemical speciation of the element of interest, e.g., the type of neighboring atoms, the coordination number, and bond lengths. The present study shows that the method is well suited to determine the local coordination of contaminants in the cement matrix such as Sr and Ni. Information on the coordination environment is essential for the development of mechanistic models of immobilization processes. The combination of SEM-BSE/EDS with synchrotron-based microXRF/XAS has proven to be a powerful approach to obtain spatially resolved micro-scale information on the interaction of Ni with specific phases of the hydrate assemblage and the chemical speciation of Ni in the cement matrix. It is shown that the latter information can only be gained by using microXRF/XAS. MicroXRF is required to determine the distribution of Ni (complemented by distribution maps of cement-derived elements) in the cement matrix in order to localize the regions of interest for microXAS measurements. The latter measurements provided the essential chemical structural information on the coordination environment of Ni. Analysis of the experimental EXAFS data, which were collected at two different spots, indicates that Ni-Al LDH are the dominant Ni containing solid phase in the cement matrix.

5 Acknowledgements

The staff of the various beamlines, 10.3.2 at the ALS, LUCIA at PSI and SNBL and DUBBLE at the ESRF, is thanked for the experimental assistance during the synchrotron-based investigations. Thanks are extended to Dr. E. Curti, D. Kunz and Dr. M. Harfouche (PSI) for assistance during the measuring campaigns. Prof. K. L. Scrivener, Dr. E. Gallucci and Dr. A. Jenni (IMX-EPFL) and R. Brüttsch (LWV-PSI) provided measuring time and experimental assistance with the SEM investigations and their contribution to this project is gratefully acknowledged. Dr. C.A. Johnson (EAWAG, Switzerland), Dr. B. Lothenbach (EMPA, Switzerland) and Dr. T. Matschei (University of Aberdeen, UK) are warmly thanked for the supply of reference compounds. Partial financial support was provided by the National Cooperative for the Disposal of Radioactive Waste (Nagra), Switzerland.

6 References

- [1] D.C. Koningsberger, R. Prins, X-ray absorption: principles, applications, techniques of EXAFS, SEXAFS and XANES, John Wiley & Sons, New York, 1988.
- [2] P.G. Allen, J.J. Bucher, M.A. Denecke, N.M. Edelstein, N. Kaltsoyannis, H. Nitsche, T. Reich, D.K. Shuh, Applications of synchrotron radiation techniques to chemical issues and environmental sciences, in: D. Amico (Ed.), Synchrotron radiation techniques in industrial, chemical, and material sciences, Plenum press, New York, 1996, pp. 169-185.
- [3] F.P. Glasser, Chemistry of cement-solidified waste forms, in: R. D. Spence (Ed.), Chemistry and microstructure of solidified waste forms, Lewis Publishers, Boca Raton, 1993, pp. 1 - 39.
- [4] A.M. Scheidegger, M. Vespa, D. Grolimund, E. Wieland, M. Harfouche, I. Bonhoure, R. Dähn, The use of (micro)-X-ray absorption spectroscopy in cement research, Waste Manage. 26 (2006) 699-705.
- [5] R.J. Kirkpatrick, G. E. Brown, N. Xu, X. Cong, X-ray absorption spectroscopy of C-S-H and some model compounds, Adv. Cem. Res. 9 (1997) 31-36.
- [6] N. Lequeux, A. Morau, S. Philippot, P. Boch, Extended x-ray absorption fine structure investigation of calcium silicate hydrates, J. Am. Ceram. Soc. 82 (1999) 1299-1306.
- [7] M. Vespa, R. Dähn, D. Grolimund, M. Harfouche, E. Wieland, A.M. Scheidegger, Micro-scale investigations of Ni uptake by cement using a combination of scanning electron microscopy and synchrotron-based techniques, Environ. Sci. Technol. (2006), in press.
- [8] E. Wieland, J. Tits, D. Kunz, R. Dähn, Strontium uptake by cementitious materials: a combined wet chemistry and EXAFS study, Environ. Sci. Technol. (in prep.)
- [9] J. Tits, E. Wieland, C.J. Müller, C. Landesman, M.H. Bradbury, A wet chemistry study of the strontium binding by calcium silicate hydrates, J. Colloid Interface Sci. 300 (2006) 78-87.
- [10] M. Vespa, R. Dähn, D. Grolimund, E. Wieland, A.M. Scheidegger, Elemental, chemical and structural information in highly heterogeneous materials: A novel approach combining synchrotron-based X-rays techniques with electron microscopic investigations, J. Microscopy (2006), submitted.
- [11] M. Janousch, A.-M. Flank, P. Lagarde G. Cauchon, S. Bac, J.M. Dubuisson, T. Schmidt, R. Wetter, D. Grolimund, A.M. Scheidegger LUCIA - a new 1-7 keV μ -XAS beamline, AIP Conference Proceedings (2004).
- [12] M. Marcus, A.A. MacDowell, R. Celestre, A. Manceau, T. Miller, H.A. Padmore, R.E. Sublett, Beamline 10.3.2 at ALS: A hard- X-ray microprobe for environmental and material sciences, Journal of Synchrotron Radiation 11 (2004) 239-247.
- [13] K.L. Scrivener, Backscatter electron imaging of cementitious microstructures: understanding and quantification, Cem. Concr. Composites. 26 (2004) 935-945.
- [14] H.F.W. Taylor, Cement Chemistry, Thomas Telford Publishing, 3rd ed., London, 1997.

